Jet Initiation of Deflagration and Detonation in Stoichiometric H_2-O_2-N_2 Mixtures

U. J. Pfahl and J. E. Shepherd

Graduate Aeronautical Laboratories
California Institute of Technology
Pasadena, CA 91125

November 2, 1999

Explosion Dynamics Laboratory Report FM99-1

Prepared for the U. S. Nuclear Regulatory Commission
for research performed under contract NRC-04-94-044

Abstract

New results are reported on the initiation of detonation in hydrogen-oxygen-nitrogen mixtures. These results were obtained at Caltech in the Hyjet facility which consists of an 1180-liter receiver vessel and a 28-liter driver vessel. Orifices of various diameters are used to connect the two vessels. The driver vessel is a 2.2-meter long tube in which combustion is initiated at the end opposite to the connection to the receiver vessel. A flame or detonation exits the driver vessel through the orifice and enters the receiver vessel, initiating combustion in the receiver vessel.

Previous work carried out in the Hyjet facility used a sensitive driver vessel mixture of 35.7% H_2, 17.9% O_2, and 46.4% N_2. Spark initiation of this mixture resulted in a detonation within the driver. The conditions under which a detonation would be initiated in the receiver vessel were measured as a function of the amount of dilution for stoichiometric hydrogen-oxygen-diluent mixtures in the receiver vessel.

In the present work, a less sensitive mixture of 20% H_2 and 80% air was used in the driver, resulting in a flame-jet entering into the receiver vessel instead of the detonation that was observed in previous tests. Critical amounts of nitrogen dilution in the receiver vessel were determined for three jet orifice diameters: 25, 64 and 92 mm and stoichiometric hydrogen-oxygen-nitrogen mixtures. The amount of diluent was measured using a parameter β equal to the molar ratio of N_2 to O_2. The critical value of beta required for prompt initiation of detonation was estimated from a series of experiments for each nozzle size. The critical value of β is estimated to be 0.4 for the 25-mm-diameter nozzle, 1.3 for the 64-mm-diameter nozzle, and 2.0 for the 92-mm-diameter nozzle. As expected, these values are substantially lower than those measured in the previous experiments that were conducted with the detonating driver mixture. In addition, the range of β for which secondary explosions (DDT) are observed in the present experiments is smaller than in the previous work in Hyjet with the detonating driver mixture.

Contents

List of Figures

List of Tables

1 Introduction

This report describes the results of testing carried out at Caltech on detonation initiation by transient flames. This is the second report on this topic; the first report (Krok 1999) describes the purpose of the experiments, a description of the facility and initial results obtained with jets produced by a detonating driver. The reader should refer to that report for a complete discussion of these aspects. For completeness, a brief summary of the earlier study is provided below.

1.1 Hyjet Facility

The purpose of the original studies (see Chapters 5 and 6 of Krok 1999) was to determine the modes of combustion created by a transient flame jet emerging into hydrogen-air-diluent mixtures. For that purpose, a facility was constructed for the study of jet-initiated deflagration and detonation. The facility is built around two pressure vessels initially separated by a diaphragm, see Fig 1. The Hyjet facility consists of an 1180-liter receiver vessel and a 28-liter driver vessel. Nozzles of various diameters are used to connect the two vessels. The driver vessel is a 2.2-meter long tube in which combustion is initiated at the end opposite to the connection to the receiver vessel. The combustion in the driver vessel may be either a low-speed flame or detonation created by the acceleration of a flame in a sensitive mixture. A high-temperature jet of combustion products exits the driver vessel through the nozzle and enters the receiver vessel, initiating combustion in the receiver vessel. The combustion in the receiver vessel can occur in a number of modes: flame-jets, deflagrations and detonations. Each of these modes was extensively examined in the previous study.

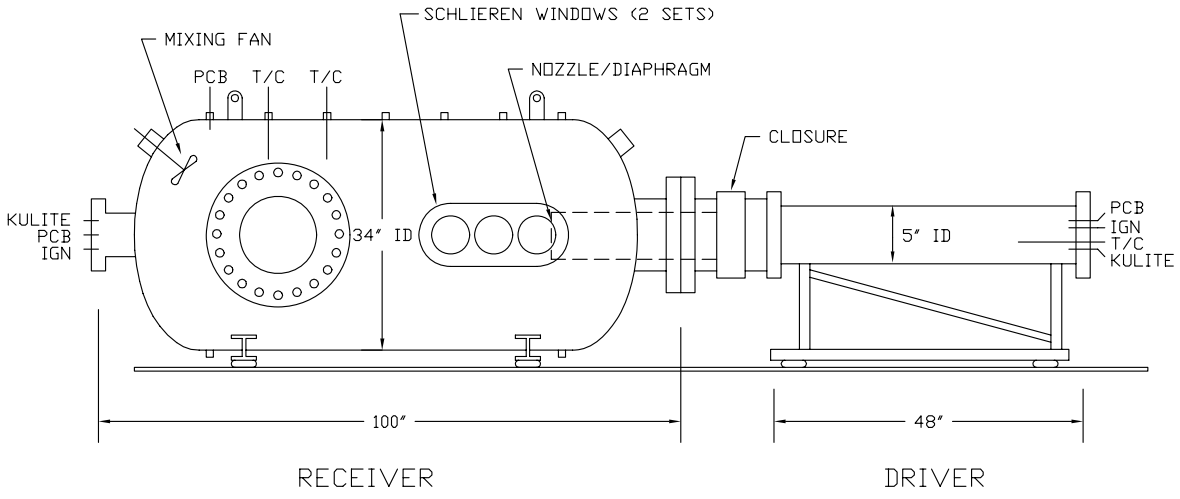

Figure 1: Schematic of HYJET facility.

1.2 Experimental Procedure

The procedure used in the present experiments is identical to that used by Krok and described in Chapter 2 and Appendix A of Krok (1999). In the present studies, the vessel was not heated so that the procedure was substantially simplified. First, the diaphragm was inserted and vessels were evacuated. After checking for leaks, the receiver was filled using the method of partial pressure with hydrogen-air and hydrogen-oxygen mixtures diluted with nitrogen. The driver gas was ignited by an electrical spark (about 40 mJ) to generate a hot mixture of combustion products. The pressure rise in the driver ruptures the diaphragm, creating a jet of hot products into the receiver vessel through the nozzle. The resulting combustion event in the receiver was determined by analyzing pressure signals from several gauges mounted in the receiver vessel.

1.3 Previous Results

The results of previous testing are described in detail in Krok (1999) and briefly recapitulated here.

The deflagration tests studied the lean and maximum-dilution limits of hydrogen-air mixtures ignited by a hydrogen-steam jet. The lean limit of 6% hydrogen was comparable to other studies. The maximum-dilution limit for steam was 60%. This is higher than the limit found in spark/glow plug ignition experiments. Shock oscillations in the receiver increased with nozzle size.

Further tests studied the initiation of detonation in both hydrogen-air and stoichiometric hydrogen-oxygen-diluent mixtures. In terms of jet diameter, D, and receiver detonation cell size, λ, we found initiation limits of $2<D/\lambda<7$, where other experiments (Bezmelnitsin et al. 1997, Carnasciali et al. 1991) required a D/λ of 11 or more. We propose that the D/λ model does not adequately characterize jet initiation, as it does not reflect the conditions in the driver. Specifically, the Mach number of the shock wave and the velocity of the jet are much larger in the case of a detonation driver than a flame driver.

The tests indicated that shock focusing plays an important role, promoting strong secondary explosions with or without prompt initiation of detonation. Mixtures with steam dilution were prone to Deflagration-to-Detonation (DDT) near the detonation limit, as the slower flame speed allows shock reflection, focusing, and pressurization to occur before the reactants were consumed. A DDT regime was not observed in the tests with nitrogen dilution over the range of dilutions that were examined. Because of DDT and shock focusing, peak pressures were highest in mixtures that were slightly less sensitive than the detonation threshold. Schlieren movies confirmed the formation of a detonation near the nozzle exit.

Previous work carried out in the Hyjet facility used a sensitive driver vessel mixture of 35.7% H_2, 17.9% O_2, and 46.4% N_2. Spark initiation of this mixture resulted in a detonation within the driver. The conditions under which a detonation would be initiated in the receiver vessel were measured as a function of the amount of dilution for stoichiometric hydrogen-oxygen-diluent mixtures in the receiver vessel. A series of tests

was carried out to determine critical nitrogen and steam dilutions, β_{crit}, of stoichiometric hydrogen-oxygen-diluent mixtures (see Fig. 8):

$$H_2 + 0.5\ (O_2 + \beta\ X\ )$$

where X is either N_2 or H_2O. These tests were carried out at initial temperatures of 298 and 373 K for N_2 and 373 K for H_2O, and an initial pressure of 1 bar in the receiver vessel. Nozzles of 25, 38, 64 and 92 mm diameter were used in these tests.

1.4 Present Study

Due to the very sensitive driver mixture (35.7% H_2, 17.9% O_2, 46.4% N_2, $\Phi = 1.0$, $\beta = 2.6$) in the initial study, DDT occurred in the driver. See the results of Fig. 5.3 in Krok (1999) and Figs. 2, 4, and 6 of this work. We speculated that this would cause the critical values of β to be lower than those that would be obtained with a flame-jet driver without DDT. That is, it would be easier to initiate detonation in the receiver with a detonation driver than with a flame driver.

In order to eliminate DDT in the driver in the present study, a less sensitive mixture of 20% H_2O and 80% air was used in the driver, resulting in a flame-jet entering into the receiver vessel instead of the detonation that was observed in previous tests. The initial pressure of the driver mixture was increased from 1.0 bar (Krok 1999) to 1.3 bar, to keep the adiabatic, isochoric, complete combustion pressure the same as in the earlier tests.

We repeated selected tests from Krok's original study using the flame driver. The amount of diluent was measured using a parameter β equal to the molar ratio of N_2 to O_2. The main purpose of the present tests was to determine the reduction in the critical value of β caused by the new driver. Only nitrogen-diluted receiver mixtures at room temperature were examined in the present study. Critical amounts of nitrogen dilution in the receiver vessel were determined for three jet orifice diameters, 25, 64, and 92 mm and stoichiometric hydrogen-oxygen-nitrogen mixtures in the receiver. The critical value of β required for prompt initiation of detonation was estimated from a series of experiments for each nozzle size.

2 Results

All tests performed as part of the present campaign are summarized in Table 1. Three different driver nozzles, 25, 64, and 92 mm diameter were investigated and the results are shown in Figs. 2–7. Two traces are shown in each figure. The top trace is from a high-speed piezo-electric pressure transducer recorded with a sampling rate sufficient to capture any shock or detonation waves. The bottom trace is from a slow-speed piezo-resistive transducer that is recorded sufficiently slowly to observe deflagrations or flames. Figs. 2, 4, and 6 show representative fast and slow pressure histories obtained in the driver while using the old driver mixture. For all three nozzle diameters, DDT is observed in the driver. The evidence of the DDT is the very rapid initial pressure rise in both the slow and fast transducers and peak pressures between 20 and 30 bar.

Figs. 3, 5, and 7 show representative fast and slow pressure histories obtained in the driver while using the new, less-sensitive, driver mixture. For shots 551 and 553, the nozzle diameter was 92 and 25 mm, respectively. In order to examine the influence of the nozzle, the extreme case of a completely sealed driver was tested in shot 550. Since only the driver behavior was of interest for these tests, the receiver was filled with air. The pressure histories obtained with a fast PCB gauge (sample rate: 150 kHz) confirm that no DDT occurs within the driver with the new mixture. The rise time of the slow pressure history is 50-100 ms in all cases and the fast pressure transducer histories show only low-amplitude (1-3 bar) shock waves.

Table 1: Data summary of hydrogen-oxygen-nitrogen mixture experiments to determine critical β-values for detonation-initiation; $p_{0,Receiver} = 1.0$ bar, $T_0 = 295$ K.

Run No.	Driver Mixture	Nozzle [mm]	Receiver Mixture H_2 %	O_2 %	N_2 %	$\beta_{Receiver}$	Receiver Prompt Detonation	DDT
544	new**	92	36.4	18.2	45.5	2.5	no	no
545	new**	92	44.4	22.2	33.3	1.5	yes	-
547	new**	92	40.0	20.0	40.0	2.0	yes	-
548	new**	92	37.7	18.9	43.4	2.3	no	no
549	old*	-	-	-	-	-	-	-
550	new**	-	-	-	-	-	-	-
551	new**	92	-	-	-	-	-	-
553	new**	25	-	-	-	-	-	-
554	new**	25	40.0	20.0	40.0	2.0	no	yes
555	new**	25	44.4	22.2	33.3	1.5	no	yes
556	old*	92	-	-	-	-	-	-
557	old*	25	-	-	-	-	-	-
558	new**	64	40.0	20.0	40.0	2.0	no	no
559	new**	64	44.4	22.2	33.3	1.5	no	yes
560	new**	64	47.6	23.8	28.6	1.2	yes	-
561	new**	25	47.6	23.8	286.	1.2	no	yes
562	new**	25	52.6	26.3	21.1	0.8	no	yes
563	new**	25	58.8	29.4	11.8	0.4	yes	-
564	new**	25	37.7	18.9	43.4	2.3	no	no

* old driver mixture: 35.7% H_2, 17.9% O_2, 46.4% N_2, $\Phi = 1.0$, $\beta = 2.6$, $p_0 = 1.0$ bar

** new driver mixture: 20% H_2, 80% air, $\Phi = 0.6$, $\beta = 3.76$, $p_0 = 1.3$ bar

The experiments used to determine the critical amount of nitrogen dilution for detonation in the receiver are given in Appendix A in Figs. 10 - 48. The position of the transducers T1, T2, T3, and E are identical to those given in Figure 6.2 of Krok (1999). Three types of results are observed in these tests. For large amounts ($\beta > 2$) of nitrogen

dilution, only a flame is observed in the receiver. This is the case in tests 544 (Figs. 19-21), 548 (Figs. 16-18), 558 (Figs. 28-30), and 564 (Figs. 46-48). The pressure signals in the receiver are characterized by slow (10-20 ms) rise times and peak pressures of less than 5 bar.

For small amounts ($\beta < 0.5$ to 1.0) of nitrogen dilution, a detonation is promptly created at the nozzle exit. This is the case in tests 545 (Figs. 10-12), 547 (Figs. 13-15), 560 (Figs. 22-24), and 563 (Figs. 31-33). The pressure signals in the receiver are characterized by rapid (1-10 μs) rise times and peak pressures of up to 30 bar.

For intermediate amounts ($0.5–1.0 < \beta < 2$) of nitrogen dilution, a delayed detonation or DDT event occurs within the receiver. This is the case in tests 554 (Figs. 43-45), 555 (Figs. 40-42), 559 (Figs. 25-27), 561 (Figs. 37-39), and 562 (Figs. 34-36). The pressure signals in the receiver are characterized by slow rise (2-5 ms) followed by a rapid (1-10 μs) jump to a peak pressure of up to 50 bar.

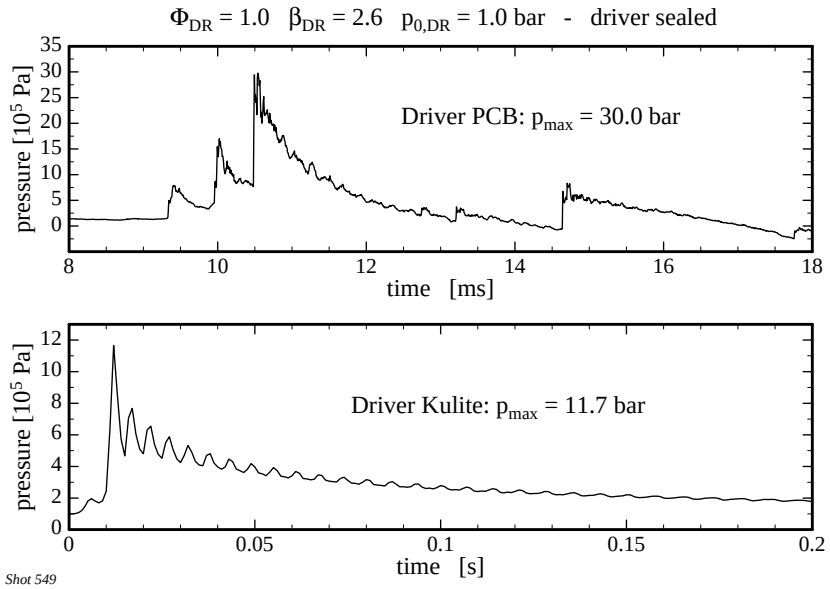

Figure 2: Test 549. Slow (Kulite pressure transducer, bottom) and fast (PCB pressure transducer, top) pressure history in sealed driver; DDT occurs in driver due to sensitive (old) H_2-O_2-N_2 driver mixture. The driver mixture parameters are given at the top of the figure: Φ_{DR} is the equivalence ratio; $p_{\circ,DR}$ is the initial pressure; β_{DR} is the nitrogen/oxygen molar ratio.

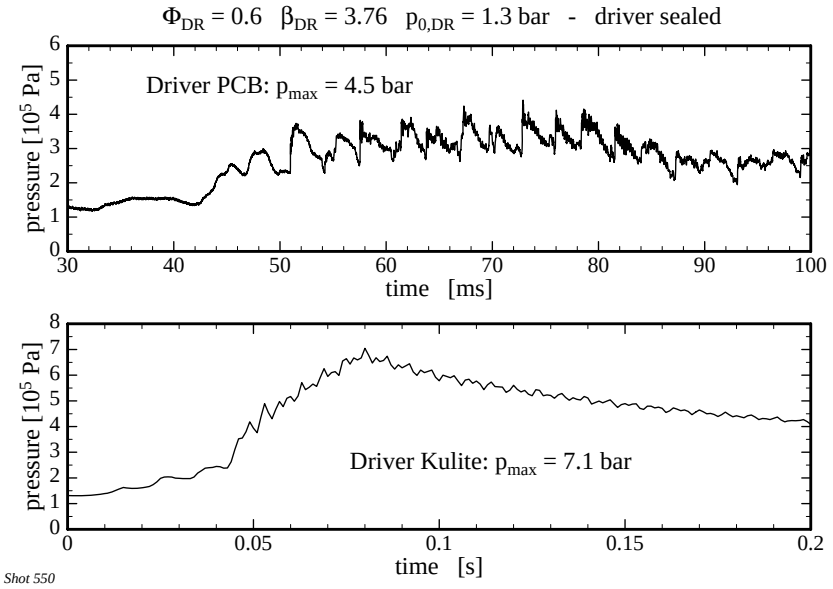

Figure 3: Test 550. Slow (Kulite pressure transducer, bottom) and fast (PCB pressure transducer, top) pressure history in sealed driver; no DDT occurs in driver due to less sensitive (new) H_2-air driver mixture. The driver mixture parameters are given at the top of the figure: Φ_{DR} is the equivalence ratio; $p_{\circ,DR}$ is the initial pressure; β_{DR} is the nitrogen/oxygen molar ratio.

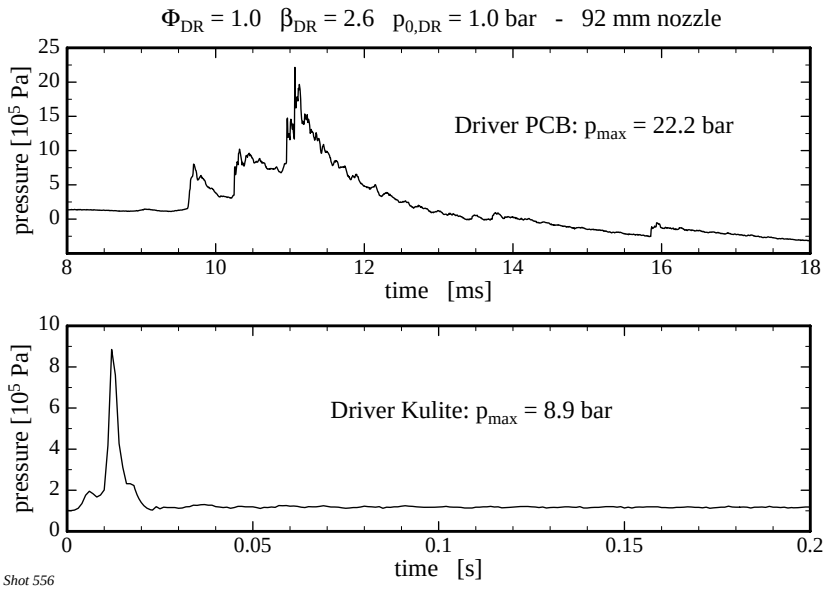

Figure 4: Test 556. Slow (Kulite pressure transducer, bottom) and fast (PCB pressure transducer, top) pressure history in driver with 92 mm nozzle; DDT occurs in driver due to the sensitive (old) H_2-O_2-N_2 driver mixture. The driver mixture parameters are given at the top of the figure: Φ_{DR} is the equivalence ratio; $p_{\circ,DR}$ is the initial pressure; β_{DR} is the nitrogen/oxygen molar ratio.

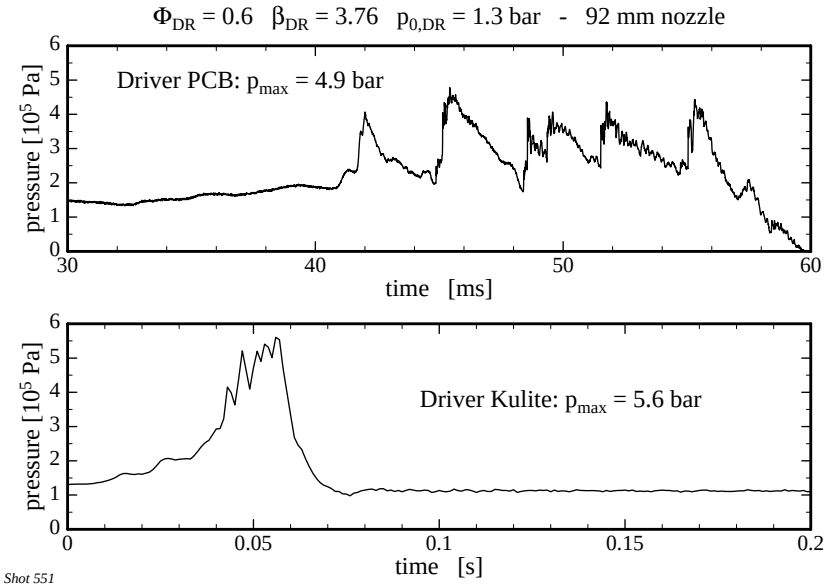

Figure 5: Test 551. Slow (Kulite pressure transducer, bottom) and fast (PCB pressure transducer, top) pressure history in driver with 92 mm nozzle; no DDT occurs in driver due to less sensitive (old) H_2-air driver mixture. The driver mixture parameters are given at the top of the figure: Φ_{DR} is the equivalence ratio; $p_{\circ,DR}$ is the initial pressure; β_{DR} is the nitrogen/oxygen molar ratio.

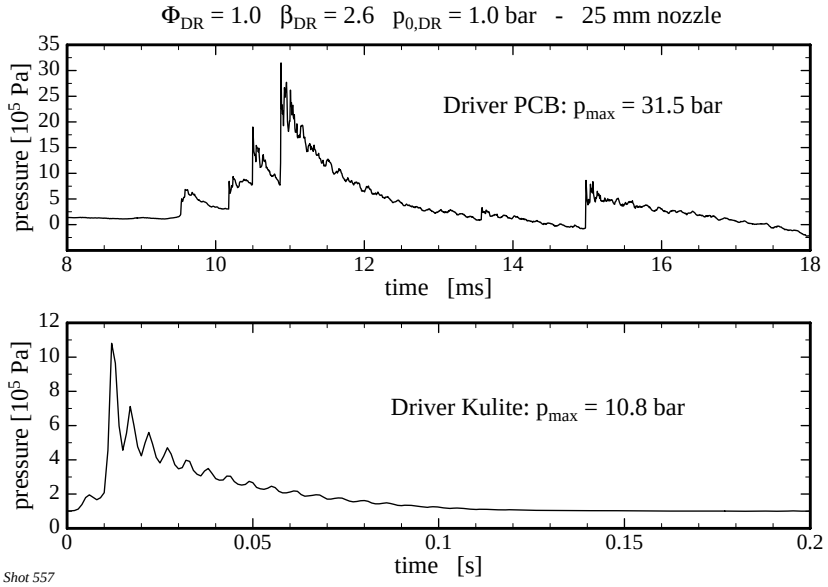

Figure 6: Test 557. Slow (Kulite pressure transducer, bottom) and fast (PCB pressure transducer, top) pressure history in driver with 25 mm nozzle; DDT occurs in driver due to the sensitive (old) H_2-O_2-N_2 driver mixture. The driver mixture parameters are given at the top of the figure: Φ_{DR} is the equivalence ratio; $p_{\circ,DR}$ is the initial pressure; β_{DR} is the nitrogen/oxygen molar ratio.

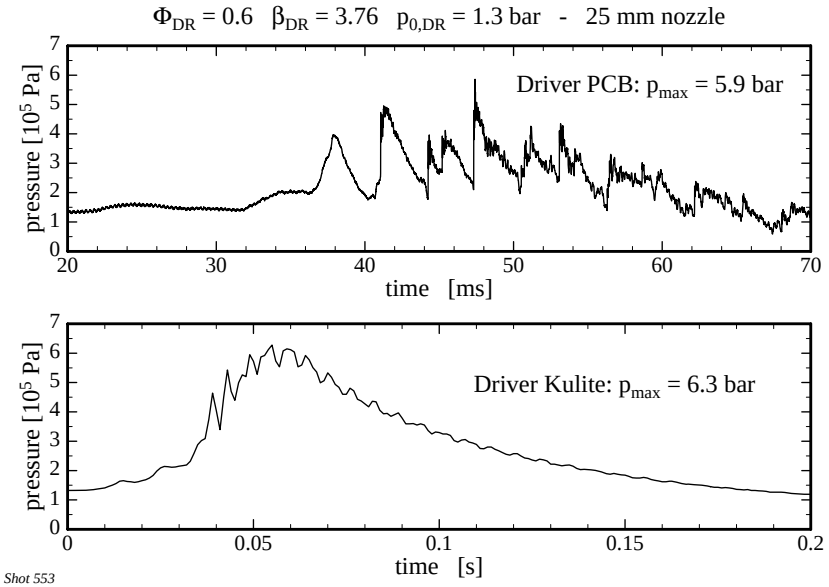

Figure 7: Test 553. Slow (Kulite pressure transducer, bottom) and fast (PCB pressure transducer, top) pressure history in driver with 25 mm nozzle; no DDT occurs in driver due to the less sensitive (new) H_2-air driver mixture. The driver mixture parameters are given at the top of the figure: Φ_{DR} is the equivalence ratio; $p_{\circ,DR}$ is the initial pressure; β_{DR} is the nitrogen/oxygen molar ratio.

3 Summary and Conclusions

Previous work carried out in the Hyjet facility used a sensitive driver vessel mixture of 35.7% H_2, 17.9% O_2, and 46.4% N_2. Spark initiation of this mixture resulted in a detonation within the driver. The conditions under which a detonation would be initiated in the receiver vessel were measured as a function of the amount of dilution for stoichiometric hydrogen-oxygen-diluent mixtures in the receiver vessel. Fig. 8 shows the original results obtained by Krok (1999) for receiver combustion regime as a function of receiver nitrogen dilution.

The results for detonation initiation as a function of receiver nitrogen dilution can be divided into the following three regions: a) For large amounts of N_2 dilution in the receiver, the combustion within the receiver proceeds completely as a deflagration, no secondary explosion (DDT) occurs in the receiver; b) For small amounts of N_2 dilution in the receiver, a prompt or direct initiation of a detonation is observed in the receiver, which propagates directly from the nozzle throughout the entire receiver mixture; c) For N_2 dilution amounts between those two limits, a secondary explosion or DDT event occurs in the receiver vessel.

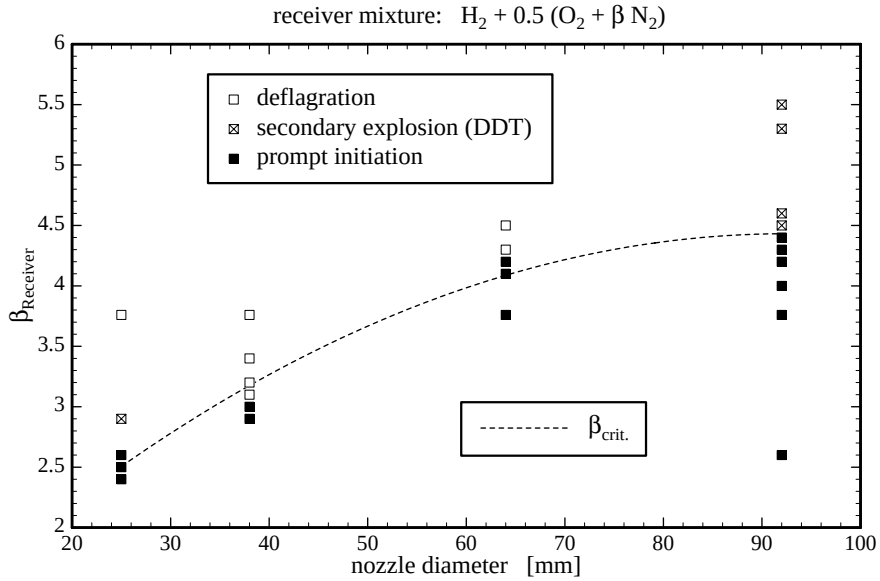

Figure 8: Summary of results for old driver (Krok 1999). Deflagration, secondary explosion (DDT), or prompt initiation of detonation in the receiver as a function of receiver nitrogen dilution $\beta_{Receiver}$.

In the present work, a less sensitive mixture of 20% H_2 and 80% air was used in the driver, resulting in a flame-jet entering into the receiver vessel instead of the detonation that was observed in previous tests. Critical amounts of nitrogen dilution in the receiver vessel were determined for three jet orifice diameters, 25, 64, and 92 mm and stoichiometric hydrogen-oxygen-nitrogen mixtures. The amount of diluent was measured using

a parameter β equal to the molar ratio of N_2 to O_2. The critical value of beta required for prompt initiation of detonation was estimated from a series of experiments for each nozzle size. The results are summarized in Fig. 9

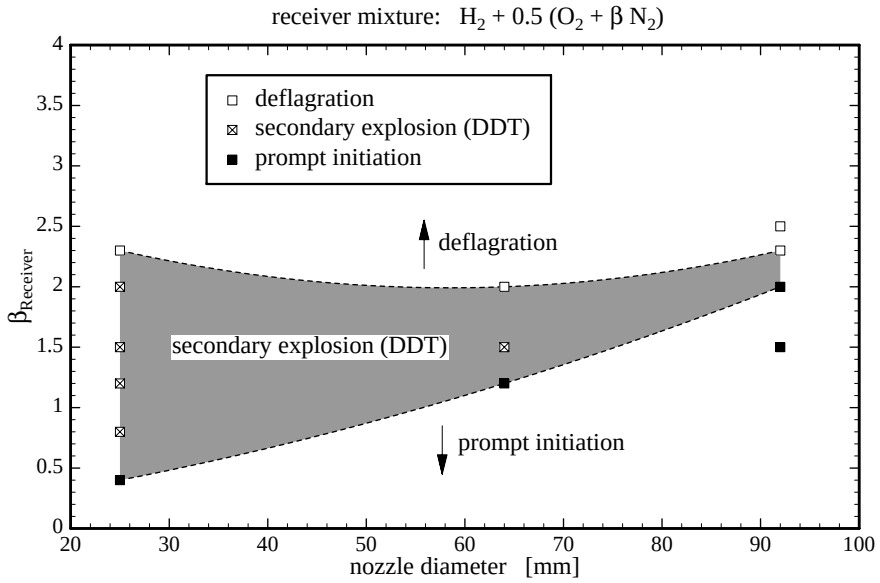

Figure 9: Summary of results for new driver mixture. Deflagration, secondary explosion (DDT), or prompt initiation of detonation in the receiver as a function of receiver nitrogen dilution $\beta_{Receiver}$.

The critical value of β is estimated to be 0.4 for the 25-mm-diameter nozzle, 1.3 for the 64-mm-diameter nozzle, and 2.0 for the 92-mm-diameter nozzle. As expected, these values are substantially lower than those measured in the previous experiments that were conducted with the detonating driver mixture. In addition, the range of β for which secondary explosions (DDT) are observed in the present experiments is larger than in the previous work in Hyjet with the detonating driver mixture. The traditional method of presenting DDT or detonation initiation data is to compare the orifice diameter to the receiver detonation cell width for the critical case. Detonation cell widths were measured at Caltech in the 288 mm detonation tube and are given in Table 2 below.

Using this data, we have analyzed our experiments and compared them with previous studies to examine the effect of facility and driver. Our conclusions are that the critical conditions for the initiation of detonation (all modes) are as follows:

- CIT (Hyjet) Detonation driver: $3 < D/\lambda < 6$
- CIT (Hyjet) Flame driver: $8 < D/\lambda < 15$
- McGill tests (flame driver): $14.8 < D/\lambda < 16.8$
- Kurchatov tests (flame driver): $18.5 < D/\lambda < 24$

Table 2: Detonation cell width λ for stoichiometric hydrogen-oxygen mixtures diluted with nitrogen at 1 bar and 295 K.

β (N_2/O_2)	λ (mm)
0.00	1.1
1.00	3.0
1.50	3.4
2.00	4.4
3.00	5.9
3.76	10.9

This comparison again illustrates that the flame driver is less effective than the detonation driver in initiating detonation in the receiver. This may be due to detonation transmission from the driver to receiver in the case of the most sensitive mixtures in the receiver. For a less sensitive mixture in the receiver, the detonation may fail when emerging from the driver and a reinitiation process may occur. A ratio of $D/\lambda = 15$ is consistent with the flame driver results in all three facilities. The details about the other facilities and an extensive discussion of detonation cell width measurement and scaling are given in Section 6.2.2 of Krok (1999).

Relevance to Severe Accident Analysis The present results indicate that the conditions (in terms of the minimum value of D/λ) required for initiating detonation through flame jets are more restrictive ($D/\lambda > 15$) than the conditions required for tranmission of a detonation through an orifice, which is usually assumed to be $D/\lambda > 13$. On the other hand, if there is a detonation creating the hot product jet, the conditions are slightly less restrictive, $D/\lambda > 6$. These results have been obtained for a limited range of jet diameters (25 to 92 mm) and for hydrogen-oxygen-diluent compositions that are much more sensitive (higher hydrogen concentrations and less diluent) than the mixtures expected in severe accident situations. In general, the conditions needed for detonation initiation by flame-jets appears to be similar to or more restrictive (more sensitive mixtures are required) than those recently proposed for DDT. The DDT criteria proposed by Dorofeev et al. (Dorofeev et al. (1997), Sidorov and Dorofeev (1998), and Dorofeev et al. (1999)) is that $L > 7\lambda$, where L is the characteristic dimension of the compartment and this is much larger than the orifice opening sizes D.

References

Bezmelnitsin, A. V., S. B. Dorofeev, and Y. G. Yankin (1997). Direct comparison of detonation initiation by turbulent jet under confined and unconfined conditions. Russian Research Centre Kurchatov Institute, Moscow, Russia.

Carnasciali, F., J. H. S. Lee, R. Knystautas, and F. Fineschi (1991). Turbulent jet initiation of detonation. *Combustion and Flame 84*, 170–180.

Dorofeev, S. B., V. P. Sidorov, W. Breitung, and A. S. Kotchourko (1997). Detonation onset scaling. In *Transactions of 14th International Conference on Structural Mechanics in Reactor Technology*, Volume 10, Lyon, France, pp. 275–283.

Dorofeev, S. B., V. P. Sidorov, M. S. Kuznetsov, I. D. Matsukov, and V. I. Alekseev (1999). Effect of scale on detonation initiation. Presented at 17th ICDERs Meeting.

Krok, J. C. (1999, January). Jet initiation of deflagration and detonation. Report prepared for the U. S. Nuclear Regulatory Commission for research performed under contract NRC-04-94-044, Explosion Dynamics Laboratory Report FM97-11, California Institute of Technology. First published in May 1997 - Revised January 1999.

Sidorov, V. P. and S. B. Dorofeev (1998, September). Detonation onset scaling. In *Proceedings of the Colloquium on Gas, Vapor, Hybrid and Fuel-Air Explosions*, Schaumburg, IL, USA, pp. 414–433. to appear in Archivum Combustionis.

A Data Plots

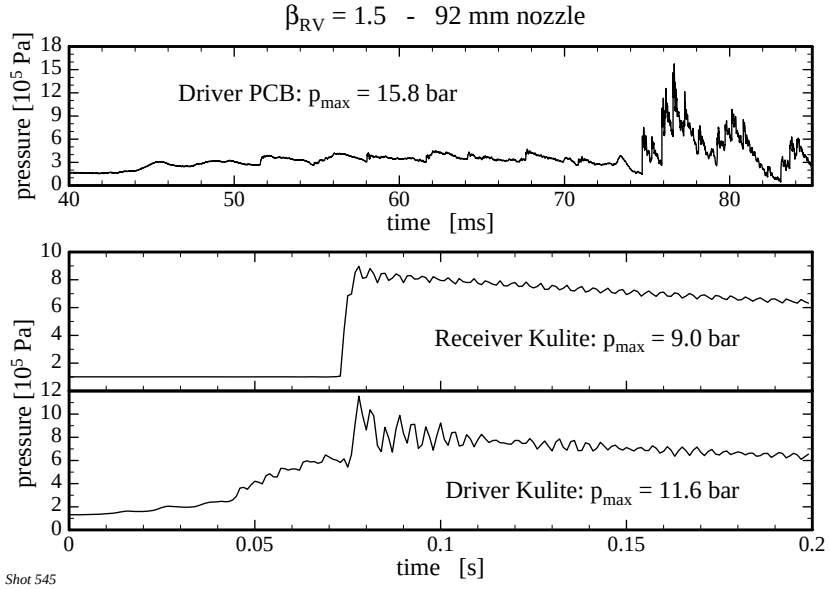

Figure 10: Test 545. Slow pressure histories (Kulite) in driver (bottom) and receiver (center); fast pressure history (PCB, top) in driver; 92 mm nozzle, $\beta_{Receiver} = 1.5$.

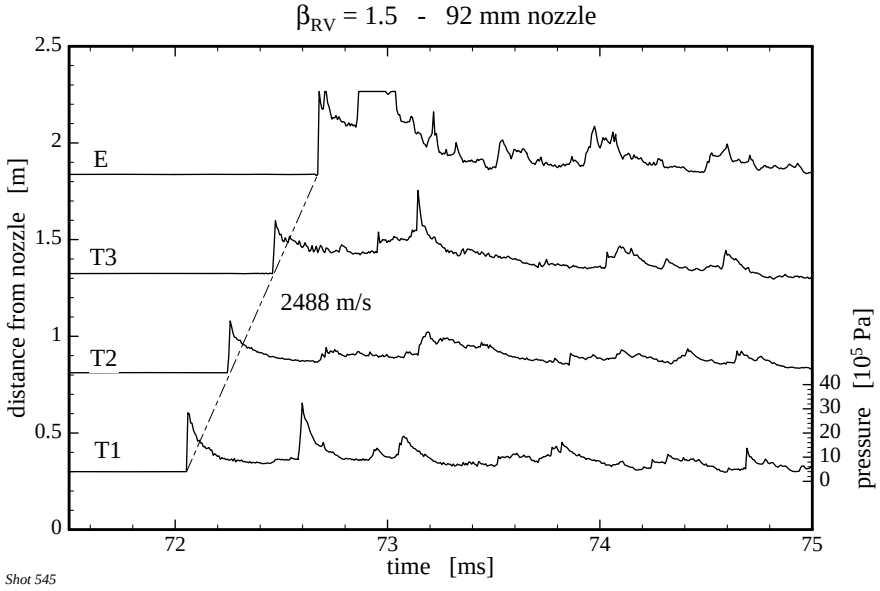

Figure 11: Test 545. Fast pressure histories (PCB) in receiver at positions T1, T2, T3 and E; 92 mm nozzle, $\beta_{Receiver} = 1.5$.

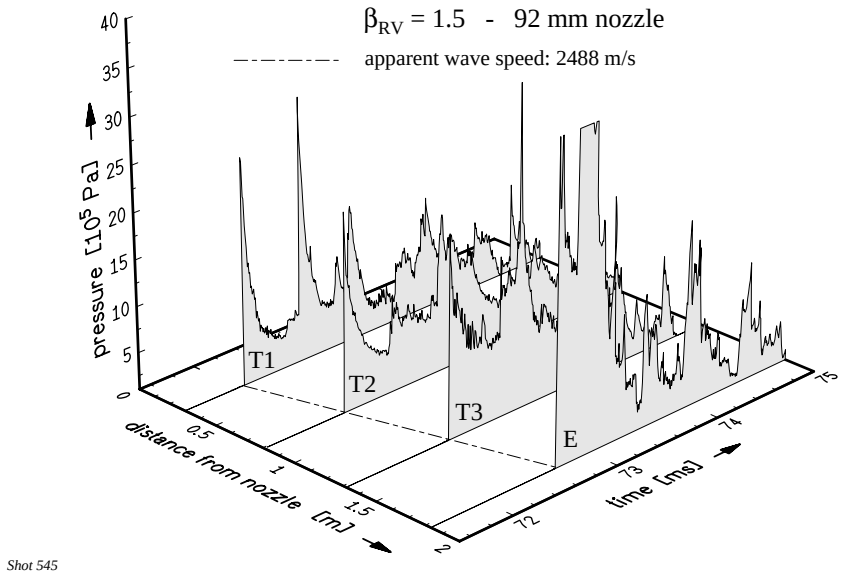

Figure 12: Test 545. Fast pressure histories (PCB) in receiver at positions T1, T2, T3 and E; 92 mm nozzle, $\beta_{Receiver} = 1.5$.

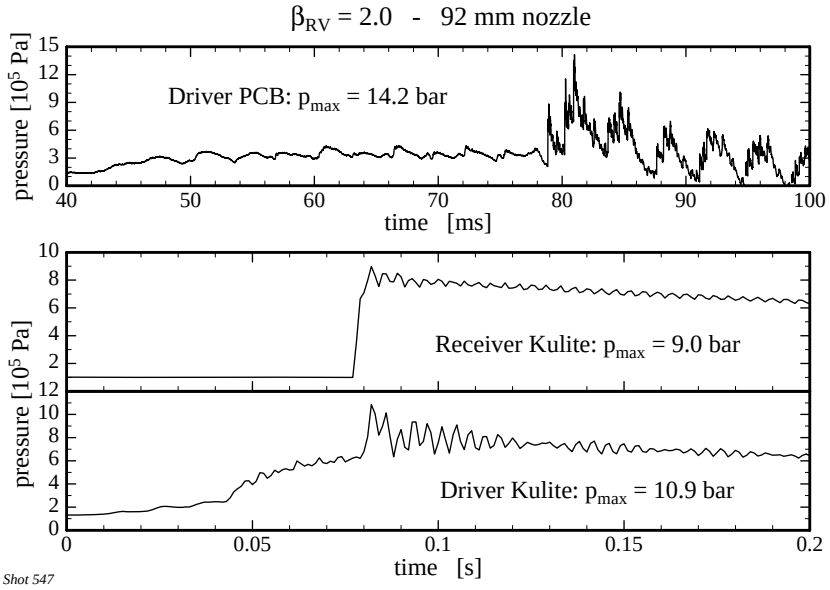

Figure 13: Test 547. Slow pressure histories (Kulite) in driver (bottom) and receiver (center); fast pressure history (PCB, top) in driver; 92 mm nozzle, $\beta_{Receiver} = 2.0$.

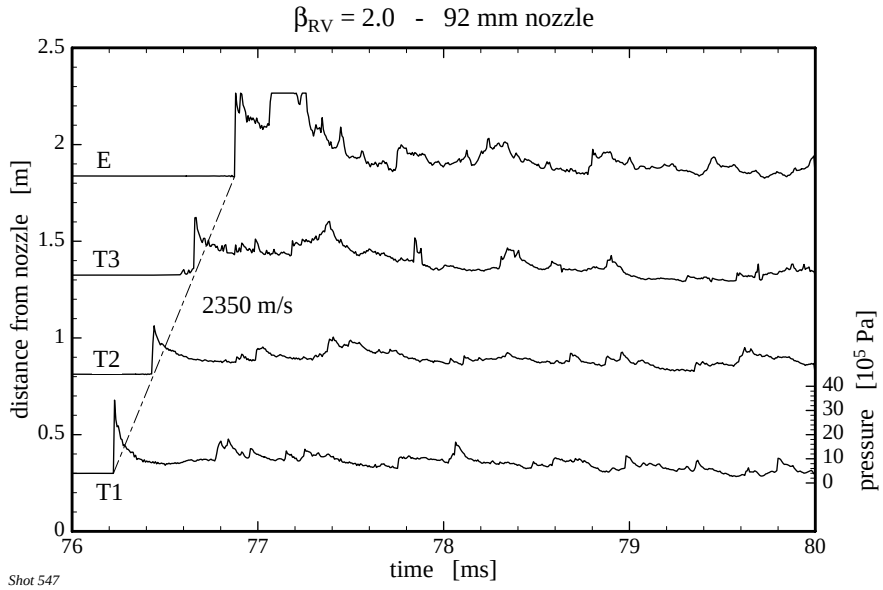

Figure 14: Test 547. Fast pressure histories (PCB) in receiver at positions T1, T2, T3 and E; 92 mm nozzle, $\beta_{Receiver} = 2.0$.

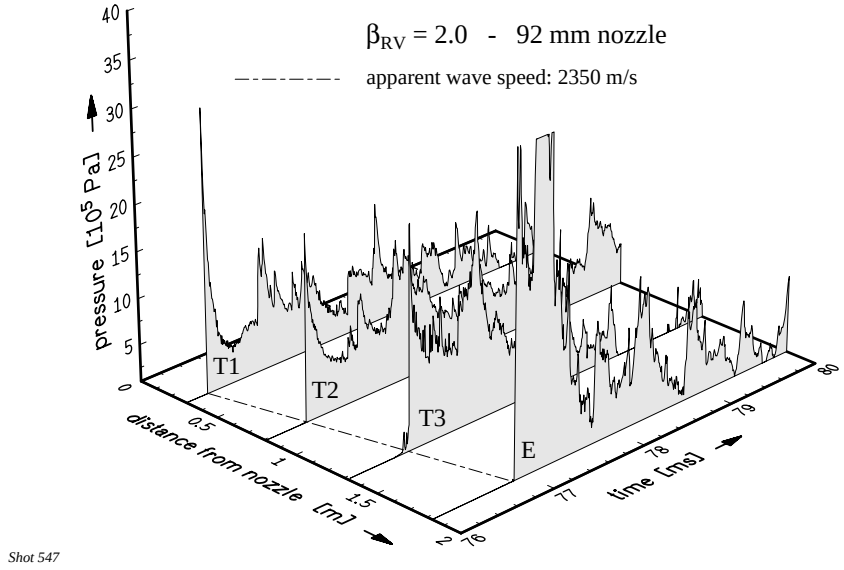

Figure 15: Test 547. Fast pressure histories (PCB) in receiver at positions T1, T2, T3 and E; 92 mm nozzle, $\beta_{Receiver} = 2.0$.

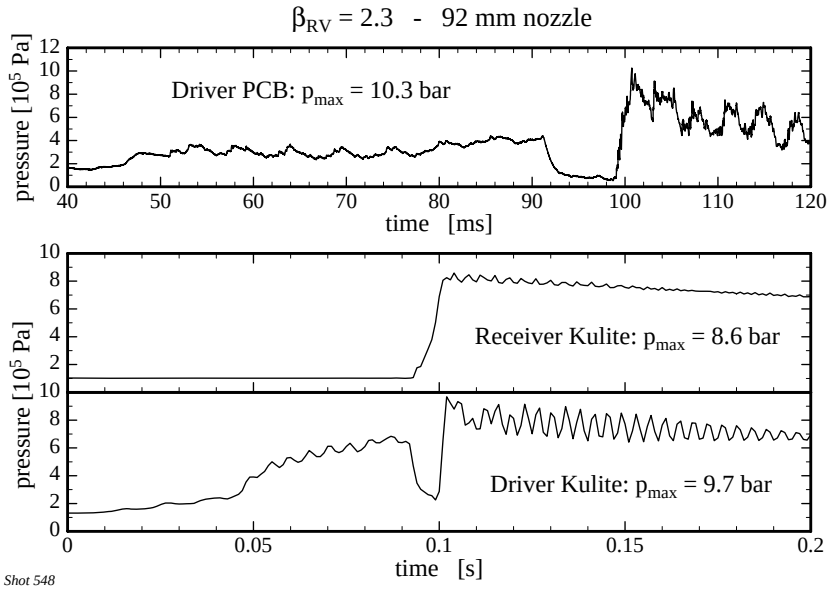

Figure 16: Test 548. Slow pressure histories (Kulite) in driver (bottom) and receiver (center); fast pressure history (PCB, top) in driver; 92 mm nozzle, $\beta_{Receiver} = 2.3$.

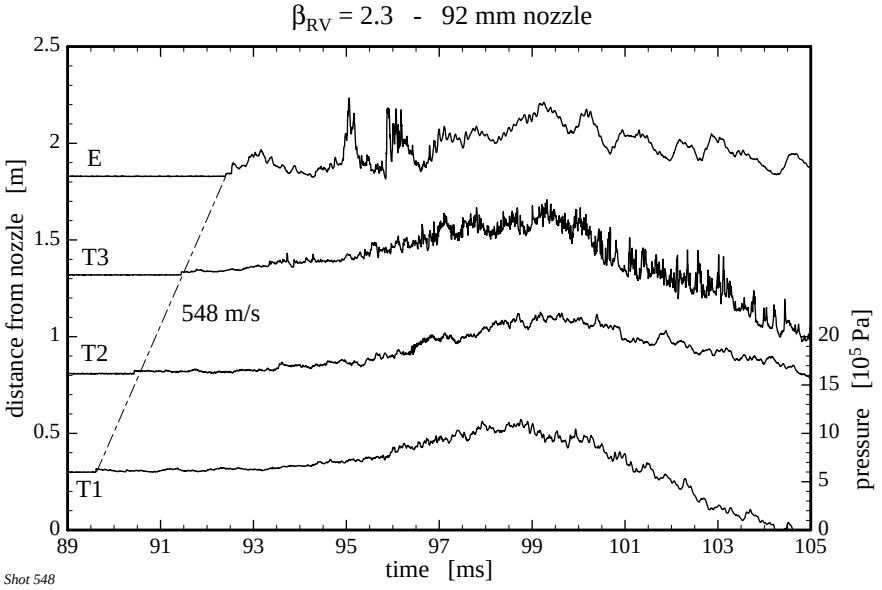

Figure 17: Test 548. Fast pressure histories (PCB) in receiver at positions T1, T2, T3 and E; 92 mm nozzle, $\beta_{Receiver} = 2.3$.

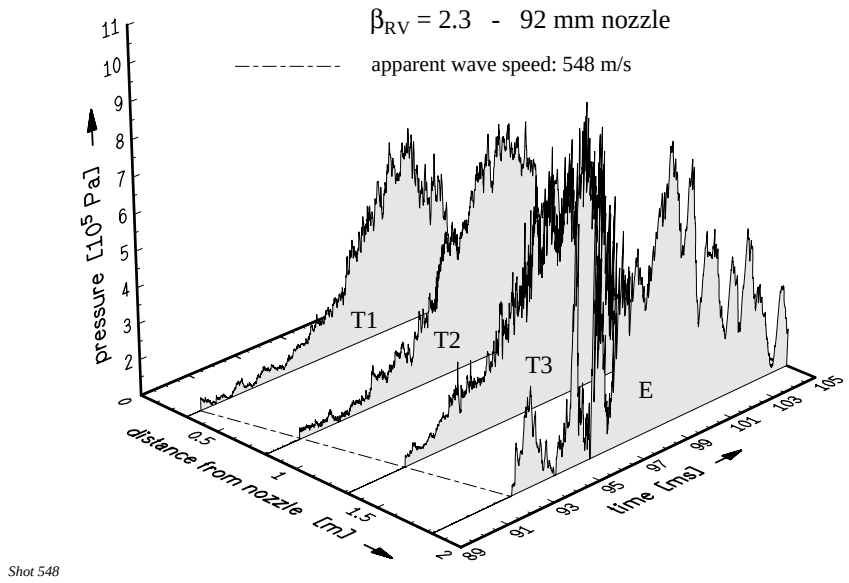

Figure 18: Test 548. Fast pressure histories (PCB) in receiver at positions T1, T2, T3 and E; 92 mm nozzle, $\beta_{Receiver} = 2.3$.

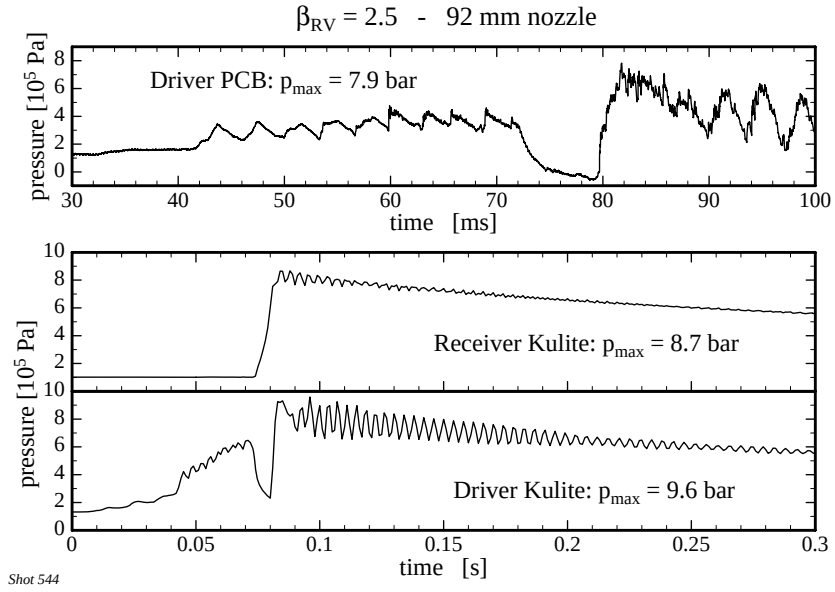

Figure 19: Test 544. Slow pressure histories (Kulite) in driver (bottom) and receiver (center); fast pressure history (PCB, top) in driver; 92 mm nozzle, $\beta_{Receiver} = 2.5$.

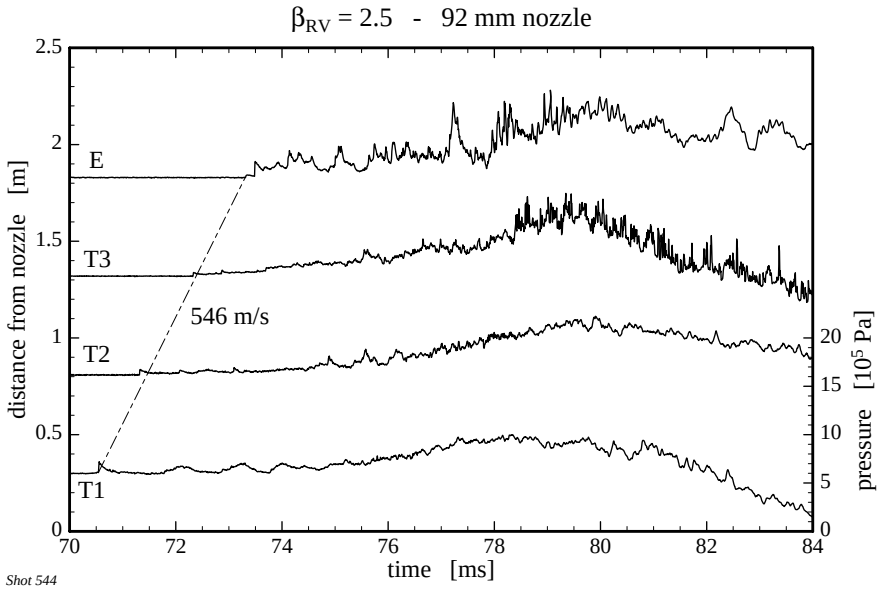

Figure 20: Test 544. Fast pressure histories (PCB) in receiver at positions T1, T2, T3 and E; 92 mm nozzle, $\beta_{Receiver} = 2.5$.

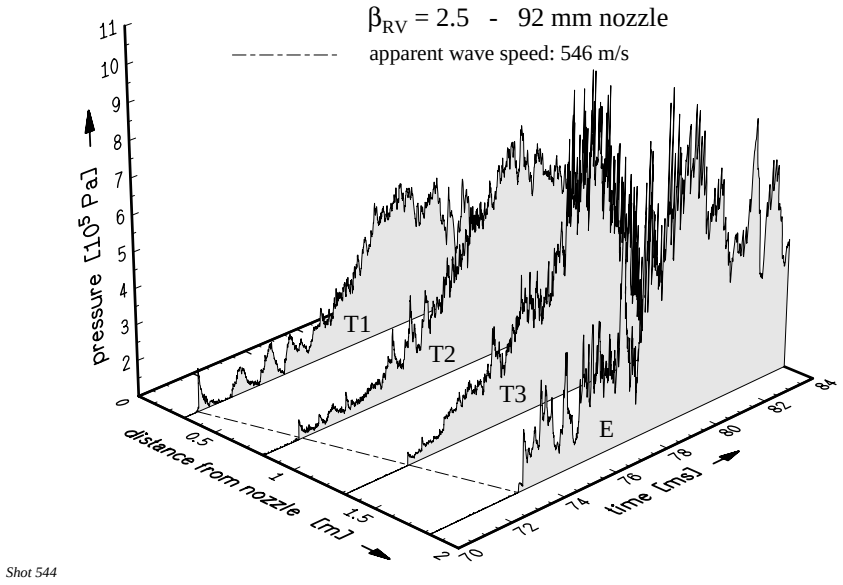

Figure 21: Test 544. Fast pressure histories (PCB) in receiver at positions T1, T2, T3 and E; 92 mm nozzle, $\beta_{Receiver} = 2.5$.

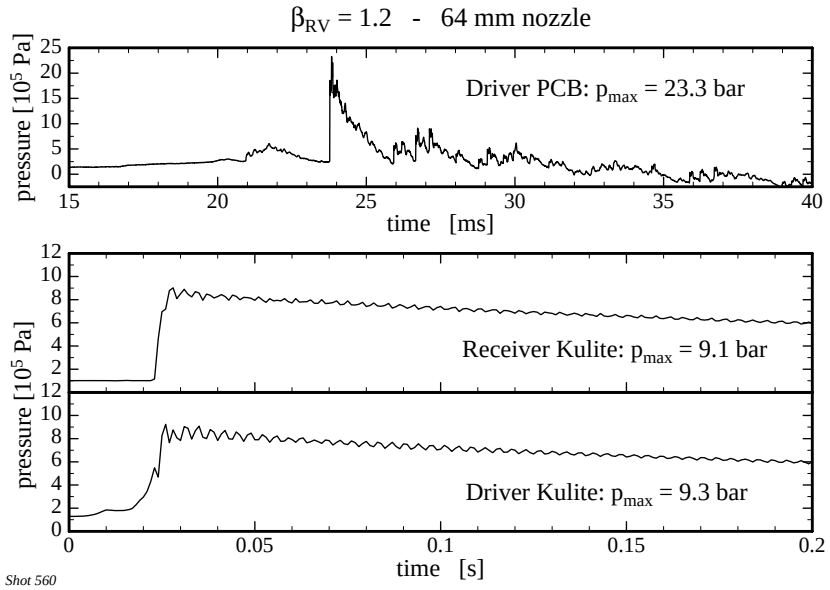

Figure 22: Test 560. Slow pressure histories (Kulite) in driver (bottom) and receiver (center); fast pressure history (PCB, top) in driver; 64 mm nozzle, $\beta_{Receiver} = 1.2$.

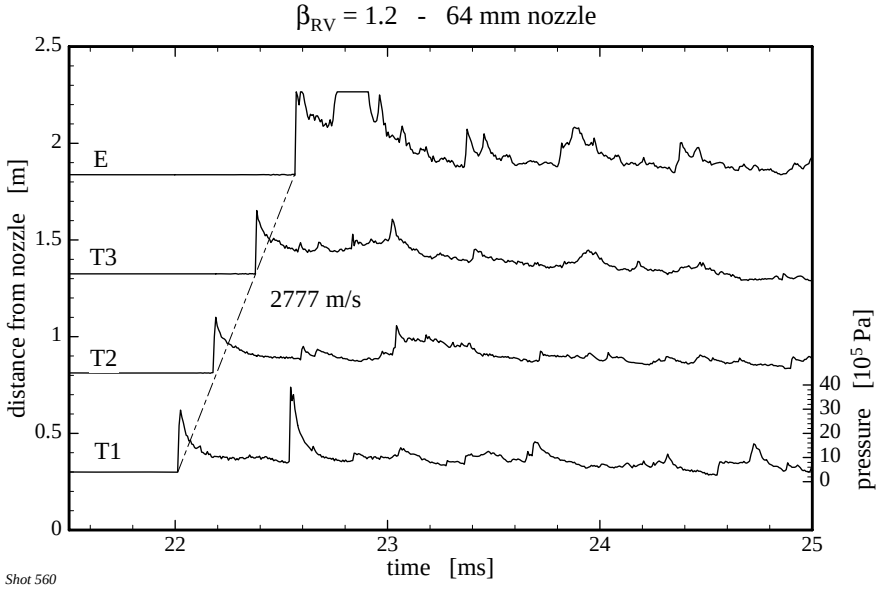

Figure 23: Test 560. Fast pressure histories (PCB) in receiver at positions T1, T2, T3 and E; 64 mm nozzle, $\beta_{Receiver} = 1.2$.

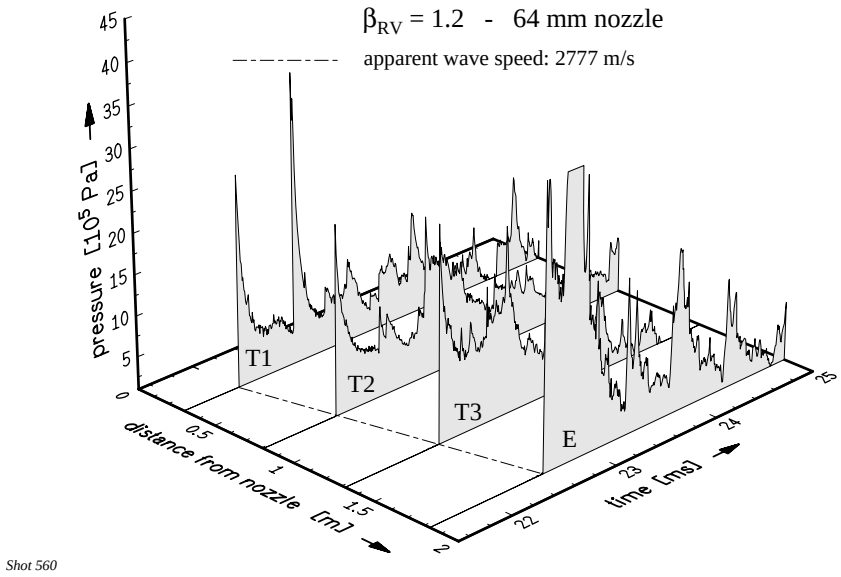

Figure 24: Test 560. Fast pressure histories (PCB) in receiver at positions T1, T2, T3 and E; 64 mm nozzle, $\beta_{Receiver} = 1.2$.

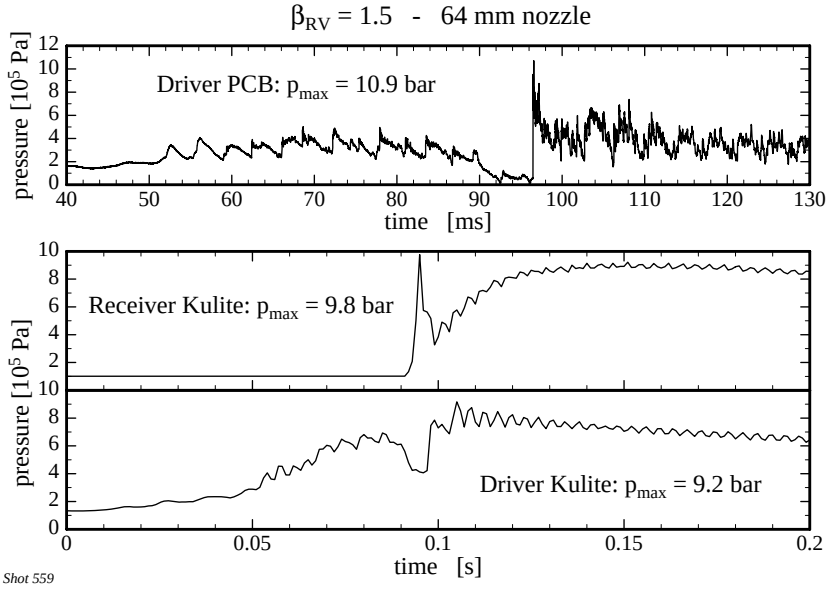

Figure 25: Test 559. Slow pressure histories (Kulite) in driver (bottom) and receiver (center); fast pressure history (PCB, top) in driver; 64 mm nozzle, $\beta_{Receiver} = 1.5$.

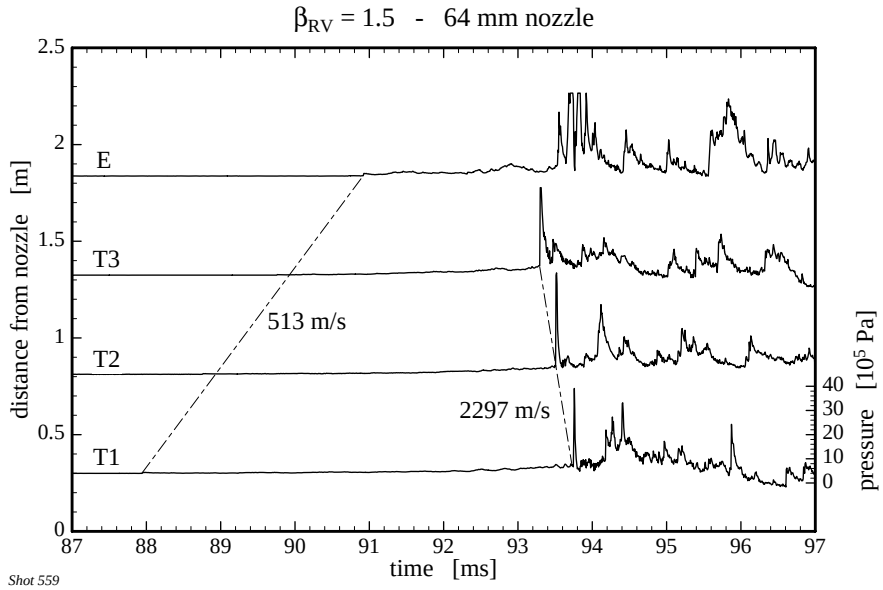

Figure 26: Test 559. Fast pressure histories (PCB) in receiver at positions T1, T2, T3 and E; 64 mm nozzle, $\beta_{Receiver} = 1.5$.

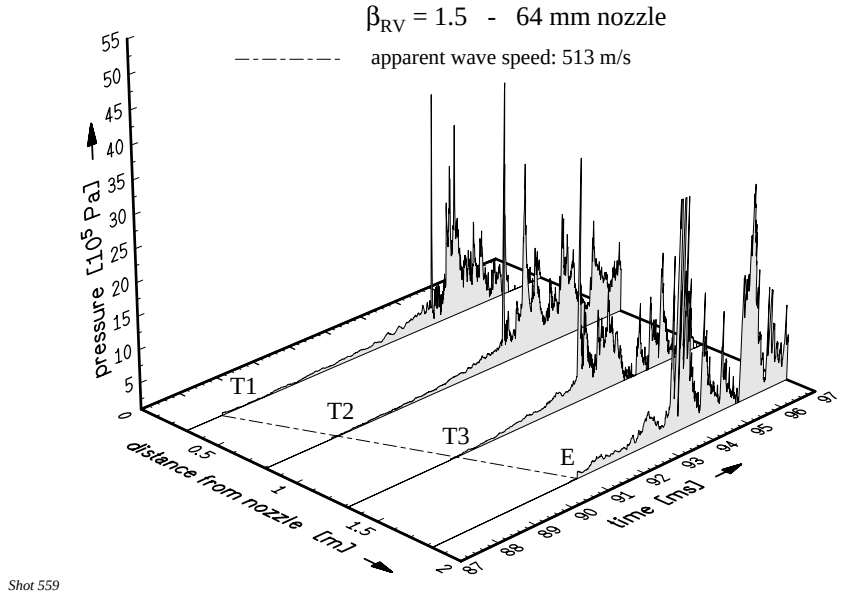

Figure 27: Test 559. Fast pressure histories (PCB) in receiver at positions T1, T2, T3 and E; 64 mm nozzle, $\beta_{Receiver} = 1.5$.

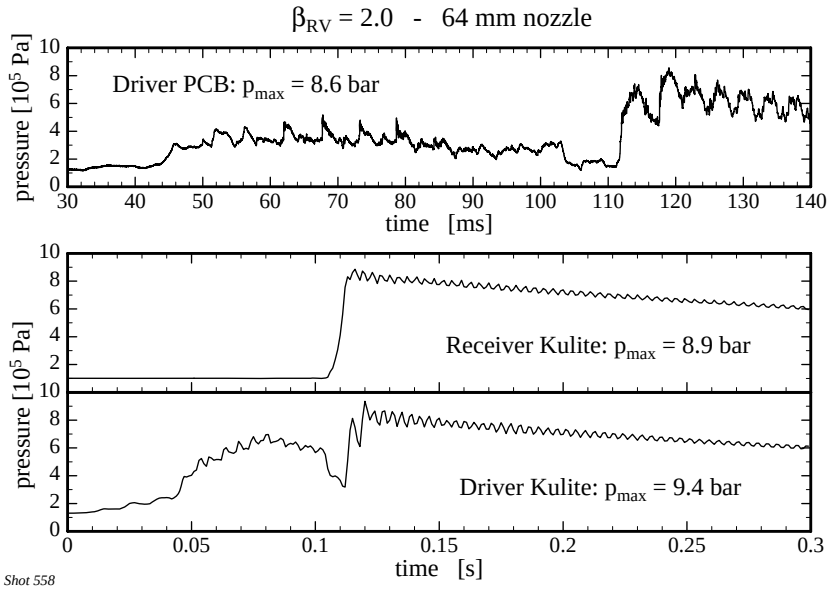

Figure 28: Test 558. Slow pressure histories (Kulite) in driver (bottom) and receiver (center); fast pressure history (PCB, top) in driver; 64 mm nozzle, $\beta_{Receiver} = 2.0$.

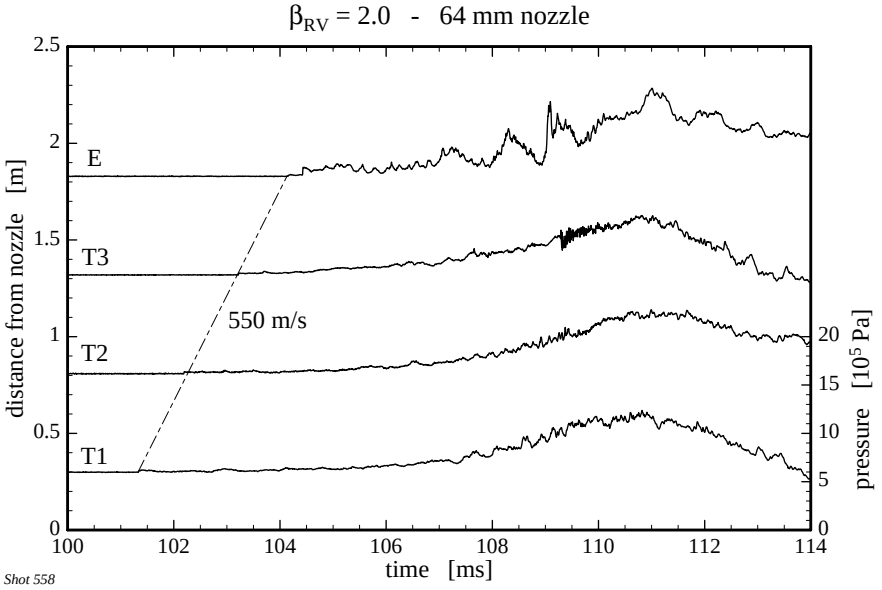

Figure 29: Test 558. Fast pressure histories (PCB) in receiver at positions T1, T2, T3 and E; 64 mm nozzle, $\beta_{Receiver} = 2.0$.

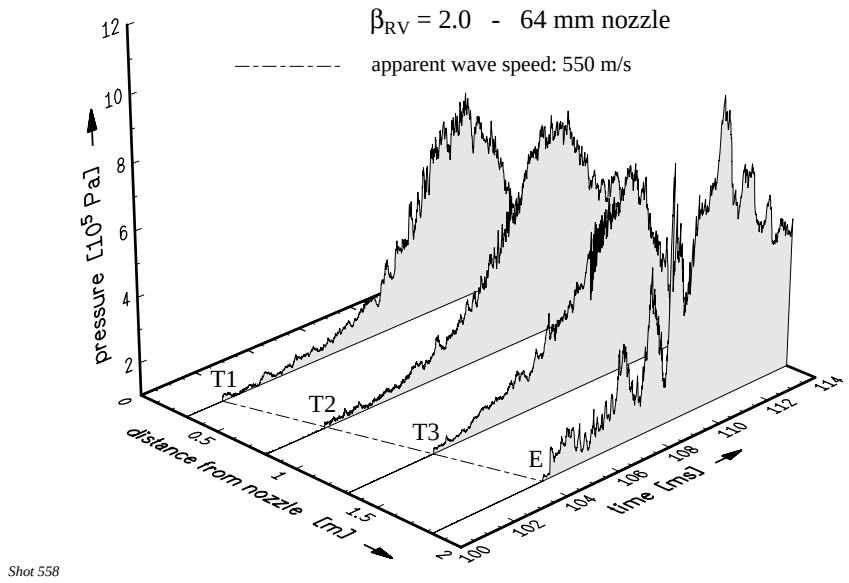

Figure 30: Test 558. Fast pressure histories (PCB) in receiver at positions T1, T2, T3 and E; 64 mm nozzle, $\beta_{Receiver} = 2.0$.

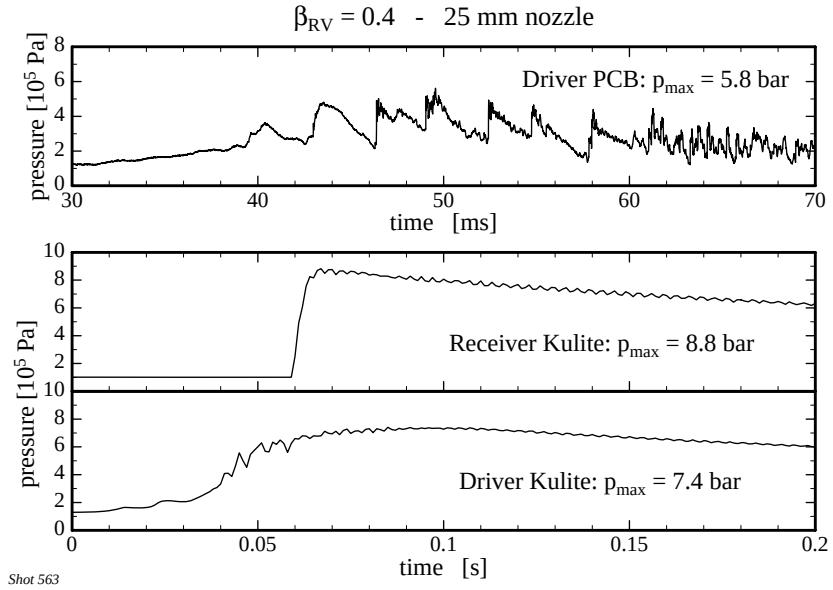

Figure 31: Test 563. Slow pressure histories (Kulite) in driver (bottom) and receiver (center); fast pressure history (PCB, top) in driver; 25 mm nozzle, $\beta_{Receiver} = 0.4$.

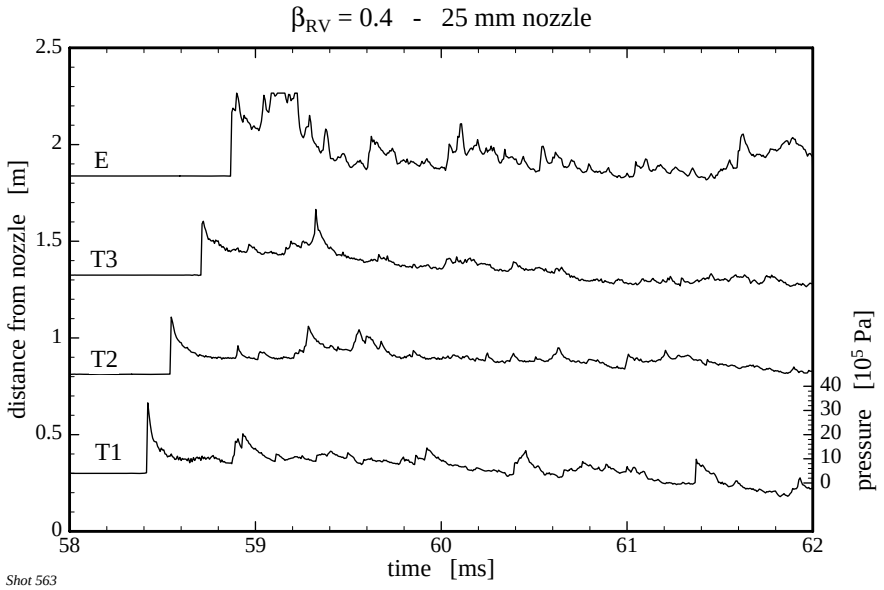

Figure 32: Test 563. Fast pressure histories (PCB) in receiver at positions T1, T2, T3 and E; 25 mm nozzle, $\beta_{Receiver} = 0.4$.

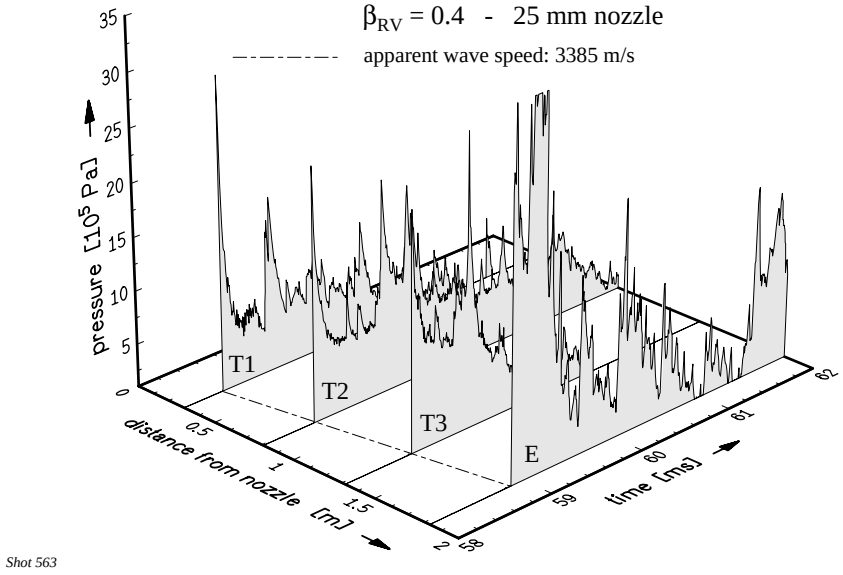

Figure 33: Test 563. Fast pressure histories (PCB) in receiver at positions T1, T2, T3 and E; 25 mm nozzle, $\beta_{Receiver} = 0.4$.

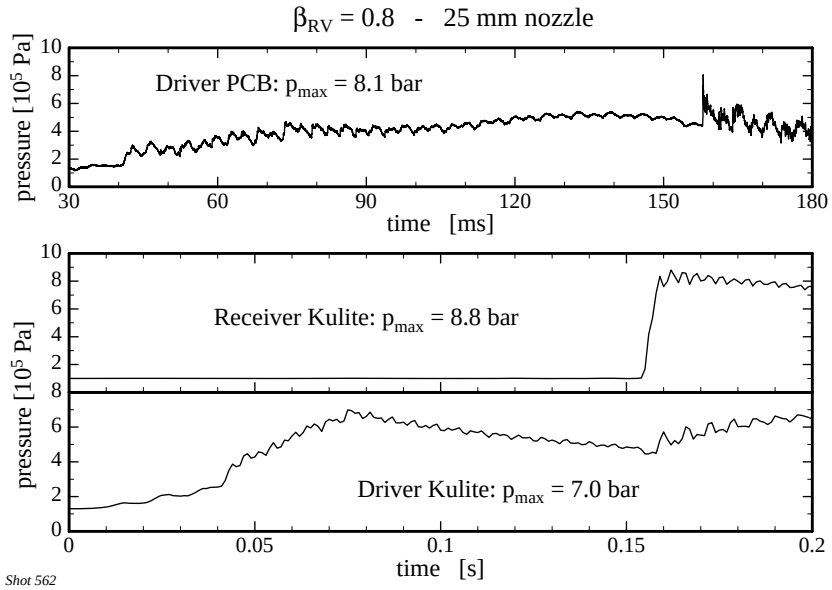

Figure 34: Test 562. Slow pressure histories (Kulite) in driver (bottom) and receiver (center); fast pressure history (PCB, top) in driver; 25 mm nozzle, $\beta_{Receiver} = 0.8$.

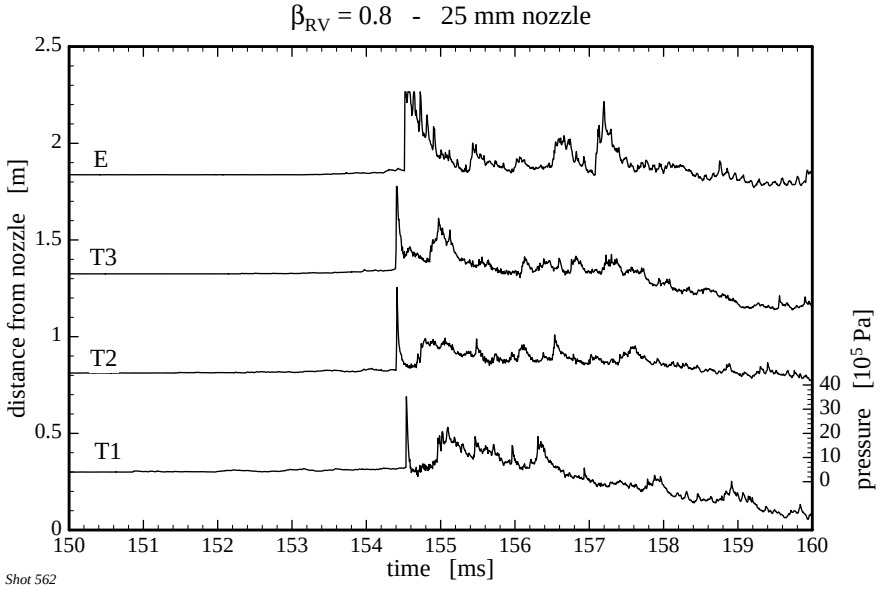

Figure 35: Test 562. Fast pressure histories (PCB) in receiver at positions T1, T2, T3 and E; 25 mm nozzle, $\beta_{Receiver} = 0.8$.

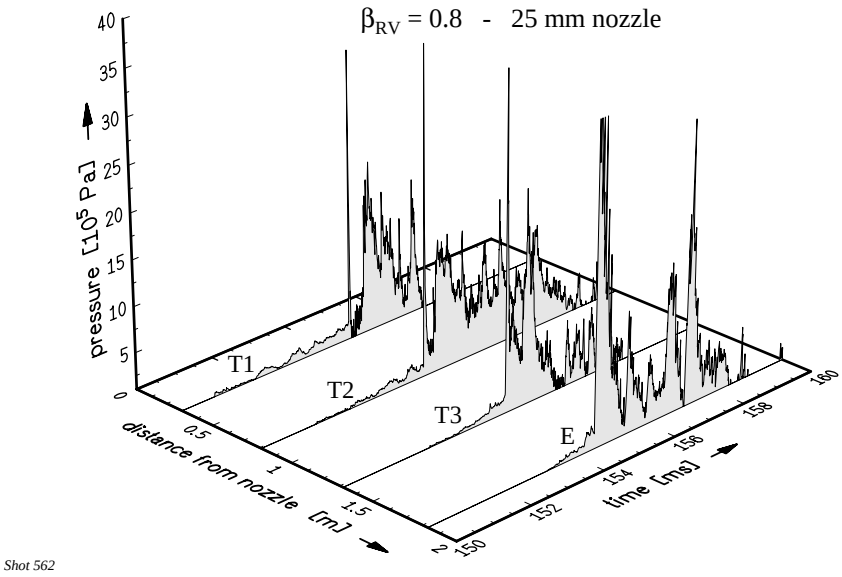

Figure 36: Test 562. Fast pressure histories (PCB) in receiver at positions T1, T2, T3 and E; 25 mm nozzle, $\beta_{Receiver} = 0.8$.

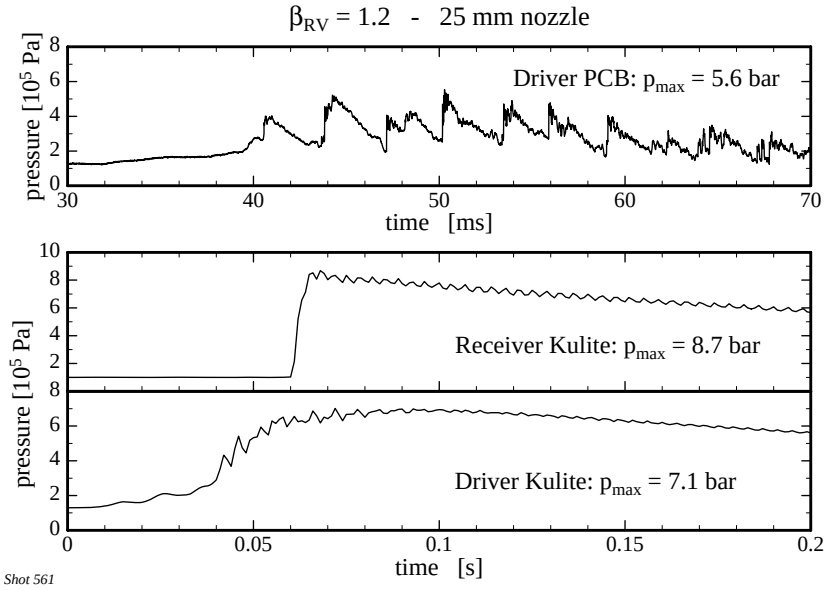

Figure 37: Test 561. Slow pressure histories (Kulite) in driver (bottom) and receiver (center); fast pressure history (PCB, top) in driver; 25 mm nozzle, $\beta_{Receiver} = 1.2$.

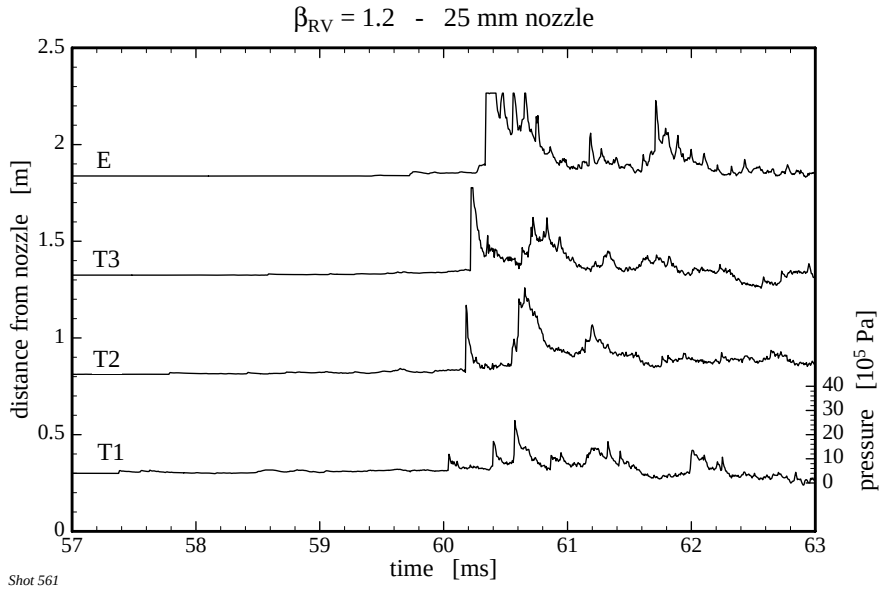

Figure 38: Test 561. Fast pressure histories (PCB) in receiver at positions T1, T2, T3 and E; 25 mm nozzle, $\beta_{Receiver} = 1.2$.

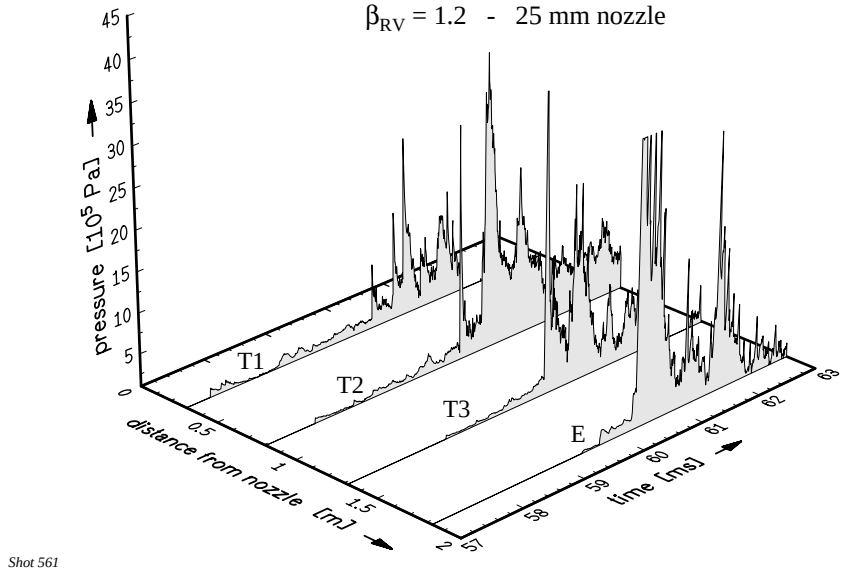

Figure 39: Test 561. Fast pressure histories (PCB) in receiver at positions T1, T2, T3 and E; 25 mm nozzle, $\beta_{Receiver} = 1.2$.

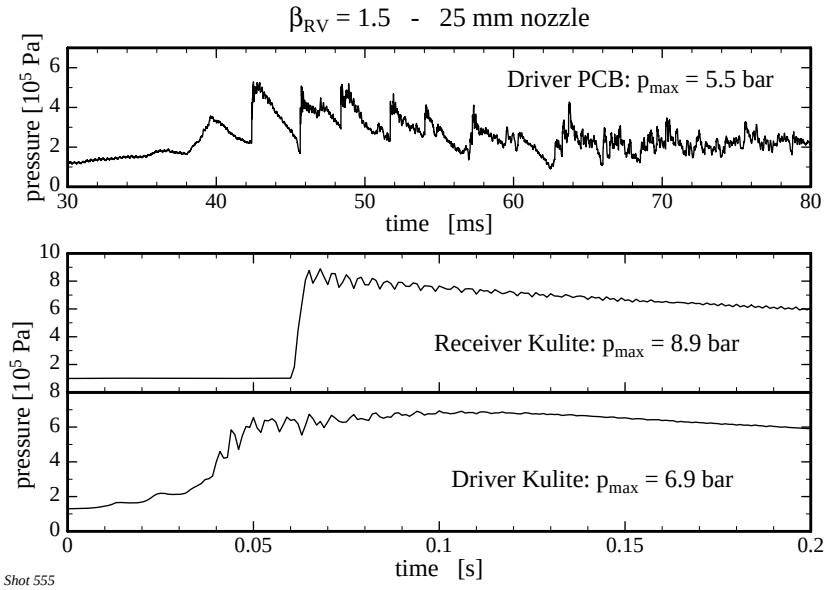

Figure 40: Test 555. Slow pressure histories (Kulite) in driver (bottom) and receiver (center); fast pressure history (PCB, top) in driver; 25 mm nozzle, $\beta_{Receiver} = 1.5$.

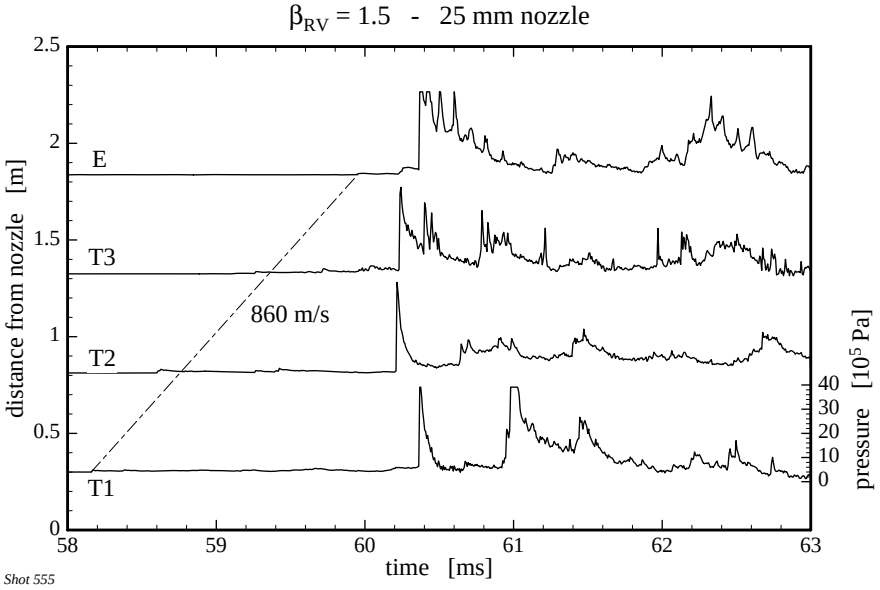

Figure 41: Test 555. Fast pressure histories (PCB) in receiver at positions T1, T2, T3 and E; 25 mm nozzle, $\beta_{Receiver} = 1.5$.

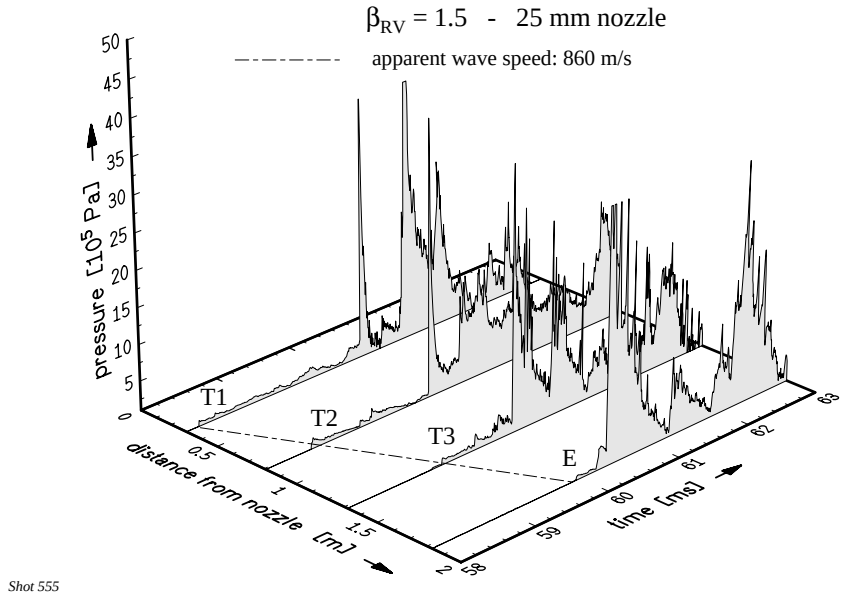

Figure 42: Test 555. Fast pressure histories (PCB) in receiver at positions T1, T2, T3 and E; 25 mm nozzle, $\beta_{Receiver} = 1.5$.

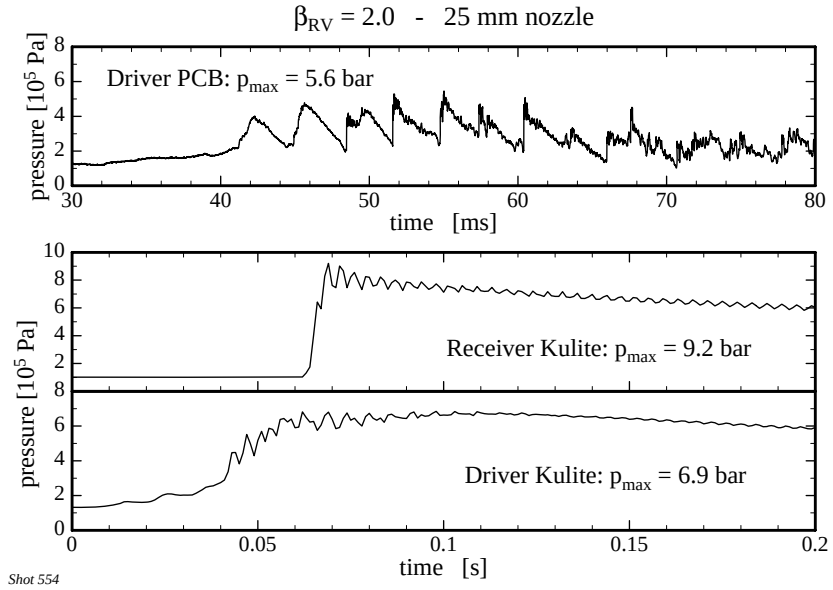

Figure 43: Test 554. Slow pressure histories (Kulite) in driver (bottom) and receiver (center); fast pressure history (PCB, top) in driver; 25 mm nozzle, $\beta_{Receiver} = 2.0$.

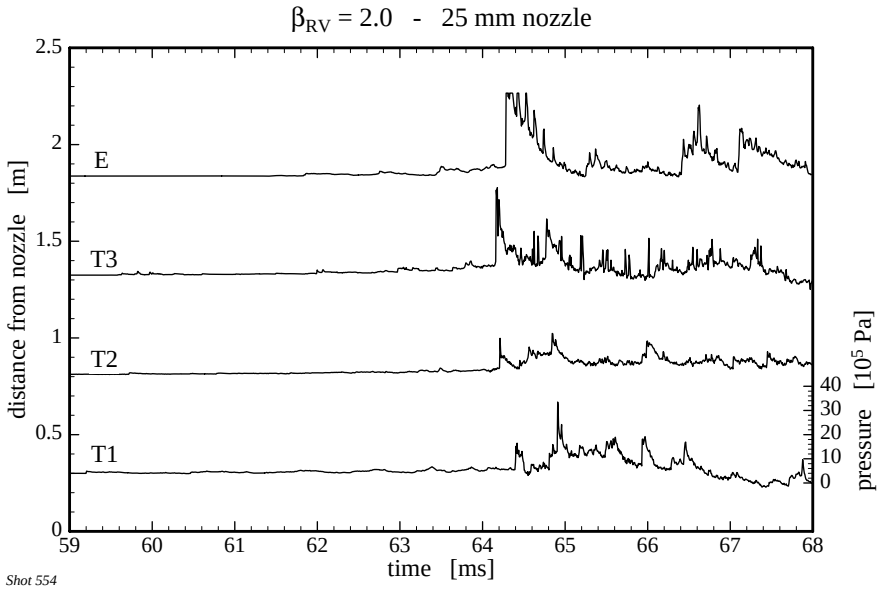

Figure 44: Test 554. Fast pressure histories (PCB) in receiver at positions T1, T2, T3 and E; 25 mm nozzle, $\beta_{Receiver} = 2.0$.

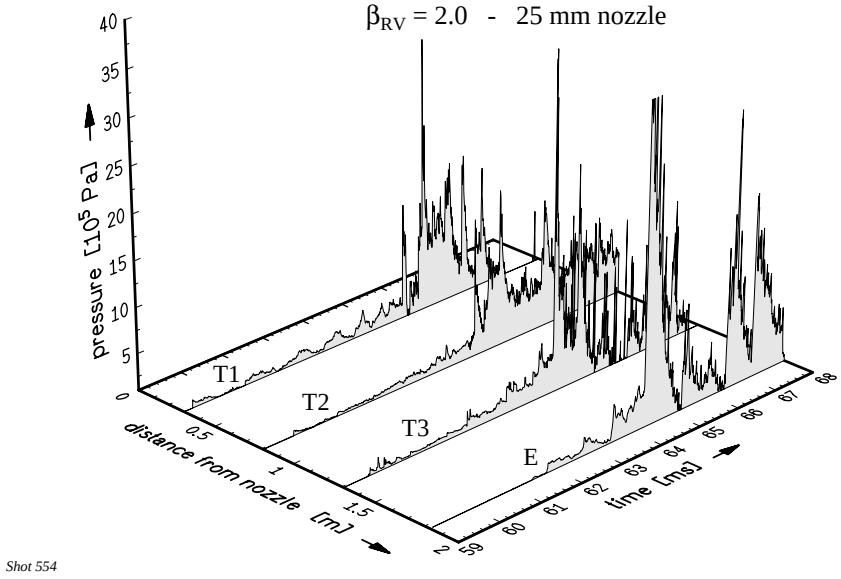

Figure 45: Test 554. Fast pressure histories (PCB) in receiver at positions T1, T2, T3 and E; 25 mm nozzle, $\beta_{Receiver} = 2.0$.

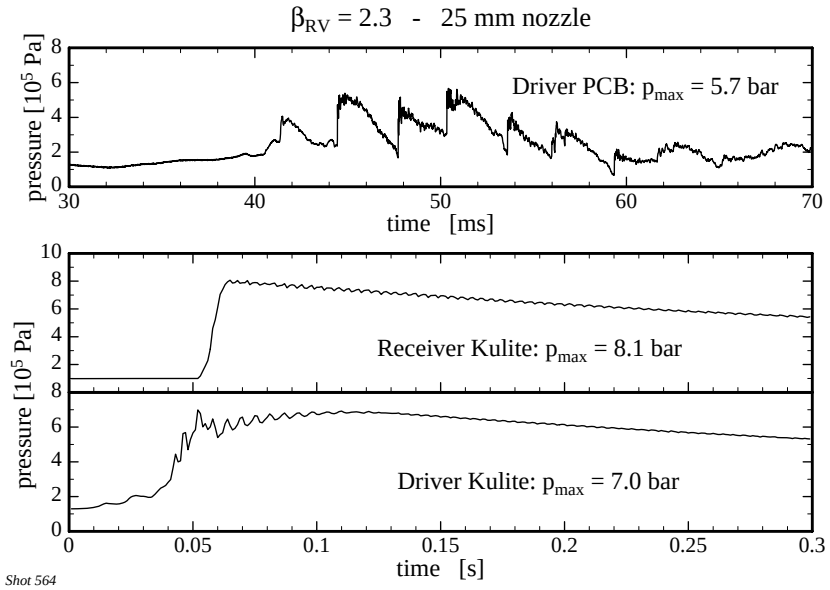

Figure 46: Test 564. Slow pressure histories (Kulite) in driver (bottom) and receiver (center); fast pressure history (PCB, top) in driver; 25 mm nozzle, $\beta_{Receiver} = 2.3$.

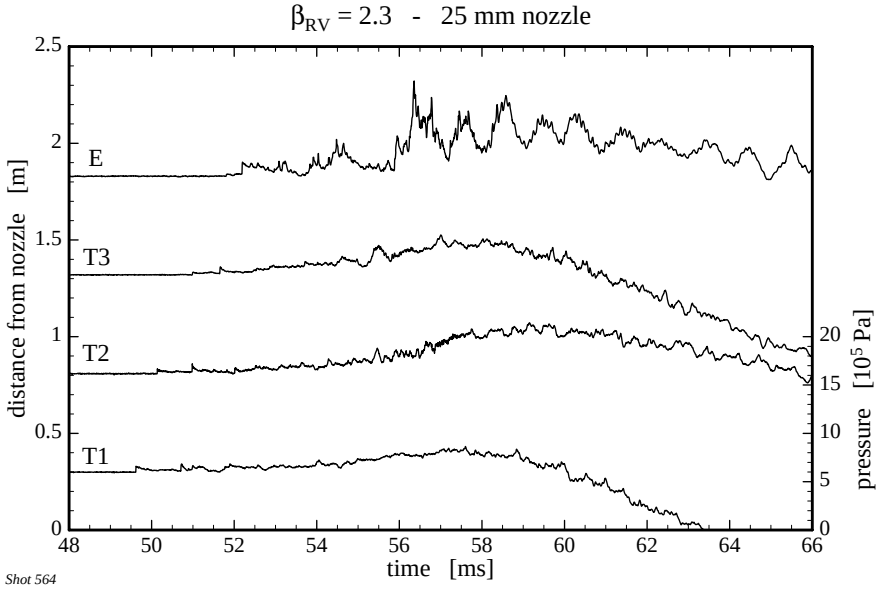

Figure 47: Test 564. Fast pressure histories (PCB) in receiver at positions T1, T2, T3 and E; 25 mm nozzle, $\beta_{Receiver} = 2.3$.

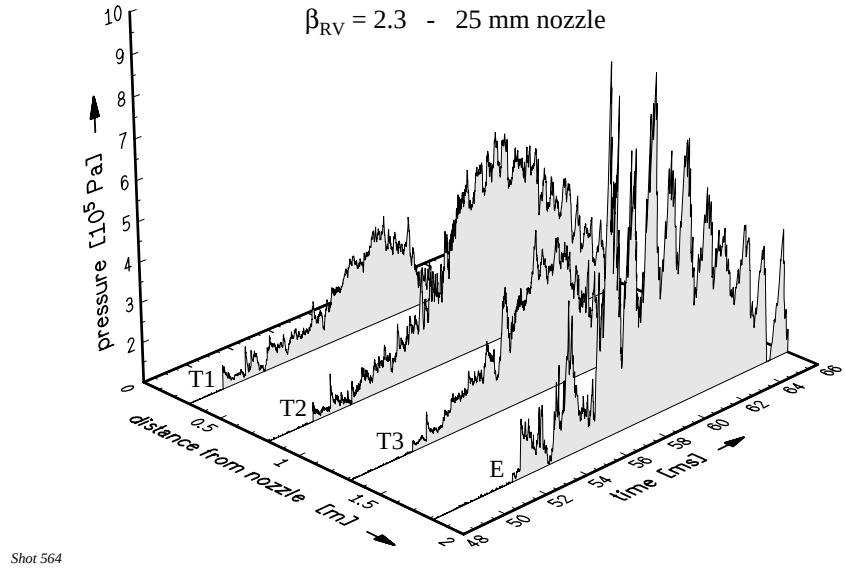

Figure 48: Test 564. Fast pressure histories (PCB) in receiver at positions T1, T2, T3 and E; 25 mm nozzle, $\beta_{Receiver} = 2.3$.